An airfoil blade in tandem cascade has a higher peak negative value of C_T in regime 3, but has a smaller range for the negative values. There is a significant increase in both the values of C_T at $\alpha = 90$ deg and the range of regime 4. This suggests that the blades in cascades have better starting characteristics than an isolated blade, but will have a lower ultimate efficiency at the operating condition.

The study of self-starting characteristics is of critical importance in determining the characteristics of a rotor subjected to sinusoidal or random oscillatory flow, where the flow may cover a range of incidences in excess of stalling angle.

Finally, some comments about testing a finite number of airfoils in a tandem cascade. It has been observed that there is no significant changes in the values of C_T and C_X for 0 deg $< \alpha <$ 20 deg, provided a minimum number of blades (say 5-7) were used for a given solidity. However, changes in the value of C_X near $\alpha = 90$ deg were observed when the number of blades in the cascade were changed, with the resulting change in end conditions. The general trend was an increase in the value of C_X with the increase in the number of blades near $\alpha = 90$ deg. Results shown here, therefore, may be a slight underestimation of C_X in regime 4.

Acknowledgment

The authors wish to thank the members of the Wave Energy Group, Queen's University of Belfast for their help.

References

[1] Wells, A. A., private communication, Queen's University, Belfast, 1976.

[2] Raghunathan, S., "Theory and Performance of Wells Turbine," Rept. WE/80/13R, Queen's University of Belfast, 1980.

[3] "Turbine Design and Application," NASA SP 290, Vol. 1, 1973.

AIAA 80-1446R

Unsteady Wake of a Plunging Airfoil

Chih-Ming Ho* and Shin-Hsing Chen†
University of Southern California, Los Angeles, Calif.

Introduction

In many engineering applications (e.g., helicopters, turbines, compressors), lifting surfaces experience unsteady motion or are perturbed by unsteady incoming flows. High level dynamic loading and noise generation are inherent problems, due to unsteadiness.[1] For example, the blades in each stage of a multistage turbine or compressor are always under the unsteady loading imposed by the unsteady wake from previous stages. This problem[2,3] is commonly referred to as "wake cutting." However, the experimental results of unsteady wakes are very limited.[4] In the present study, the multiple hot-wire probe measurements and the on-line data acquisition system have significantly facilitated the study of an unsteady wake. Several interesting features of the wake of a plunging airfoil are presented in this Note.

Presented as Paper 80-1446 at the AIAA 13th Fluid and Plasma Dynamics Conference, July 14-16, 1980; submitted Sept. 24, 1980; revision received April 17, 1981.

*Associate Professor, Dept. of Aerospace Engineering. Member AIAA.

†Research Assistant, Dept. of Aerospace Engineering. Student Member AIAA.

Experimental Setup

The experiments were conducted in a low turbulence ($u'/U_0 < 0.02\%$) wind tunnel. The flow speed of the tunnel was varied from $U_0 = 2.5$ to 40 m/s. The airfoil used in the experiment has a NACA 0012 profile. The airfoil was molded from a high strength aluminum filled epoxy (DEVCON F2). The chord of the airfoil is $c = 10$ cm and the span is 53 cm. A pair of end plates was added on the airfoil in order to achieve two-dimensionality of the flow.

The driving mechanism of the plunging airfoil has a simple and versatile design, consisting of a dc motor, gears, eccentric wheels, and two shafts. The motor and gear combination can provide a wide variation of oscillation frequencies f. The maximum frequency is 20 Hz. The oscillation amplitude, determined by the eccentricity, is 0.32 cm. A phase referencing device is attached to the mechanism. An assembly consisting of a light source and a photo-transistor detects the passage of the driving gear and provides the triggering signal necessary in data reduction.

A miniature hot-wire rake was made to survey the flow. There are 10 hot-wires (five X-wires) on the rake. Each X-wire comprises two wires in X-array. The streamwise and transverse velocities could be measured by an appropriate combination of the angular sensitivities of the two cross wires. The cross section of each X-wire is 1.0×1.4 mm. The hot-wire rake is mounted on a traverse mechanism with three degrees-of-freedom. The movement in each direction is driven by a stepping motor that is controlled by a computer. All 10 hot-wire outputs were directly connected to the analog-digital converter interfaced to a PDP 11/55 minicomputer. The triggering signal was digitized with the hot-wire outputs and provided a phase reference for conditional sampling and ensemble averaging.

Experimental Results

In the investigation of the near wake of the plunging airfoil, 10 test cases covering a wide range of operating parameters were performed. The Reynolds number, $Re = U_0 c/\nu$, was varied from 2.1×10^4 to 10^5. The reduced frequency, $k = \omega c/2U_0$, was varied from 0 (stationary airfoil) to 1. Here ω is the angular frequency, $\omega = 2\pi f$. The angle of attack, θ, is 5 deg in all tests.

The instantaneous streamwise and transverse velocity components, u and v, are displayed in Fig. 1. A triggering pulse train is provided by a phase reference device on the driving mechanism. The triggering pulse in Fig. 1 indicates the time when the airfoil is at the lowest position during the oscillation. Features in the unsteady wake can be "visualized" simultaneously at several points across the entire wake. There are distinctly different characteristics in the upper and lower portions of the wake. The hot-wires located in the lower portion of the wake are intermittent inside and outside the

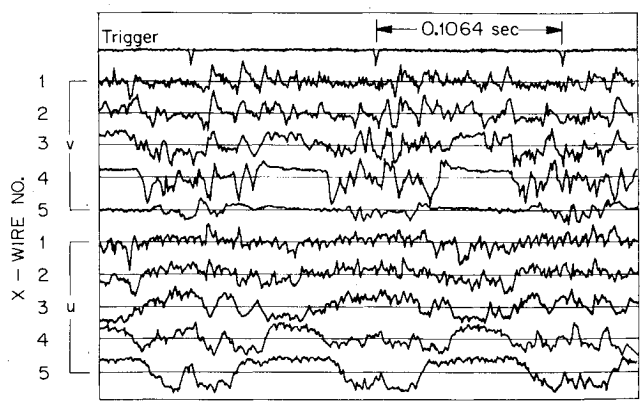

Fig. 1 Time record of velocity traces.

viscous wake, so the signals have sharp interfaces. High level turbulence is usually developed along the upper side of the airfoil and shed downstream to form a much dispersed wake in the transverse direction. Hence, the signal in the upper wake is less intermittent. The fourth X-wire in Fig. 1 is located near the position where the airfoil has zero mean transverse displacement, while the third and the fifth X-wires are located at the uppermost and the lowest positions of the plunging airfoil, respectively. The streamwise velocity traces of the third and fifth wires are therefore out of phase between these two X-wires, as shown in Fig. 1. The highest transverse velocity fluctuations in the whole wake appear near the position where the airfoil has zero mean displacement. Apparently, the oscillation of the airfoil is the main cause, because the airfoil has maximum transverse velocity at the zero mean transverse displacement location.

The mean streamwise velocity distribution has an approximately asymmetric, bell-shaped profile. The half wake width, $y_{1/2}$, is defined as the distance between two points where the mean velocity is half the velocity defect, $U_0 - U_{\min}$. An interesting point, found in Fig. 2, is that the streamwise velocity defect does not approach zero within a short distance from the center of the wake. The nonzero velocity defect extends to about one chord length away from the trailing edge with a small velocity gradient. Actually the wake consists of a viscous part and an inviscid part. The viscous wake is the result of the merging of two boundary layers on the airfoil. The viscous wake has high velocity gradient and high turbulence levels,[5] and is limited in a very thin region due to the high Reynolds number. The inviscid wake is due to the presence of the airfoil in the flow with a nonzero angle of attack. Though the magnitude of the velocity defect is small, the width is large. The momentum deficit of the inviscid wake is appreciable. In the wake of a steady airfoil, a similar velocity profile was observed in the present measurement. The mean transverse velocity is difficult to resolve from the measured hot-wire signals since it is only a few percent of the mean streamwise velocity. The mean transverse velocity was accurately measured by using a refined calibration procedure (Fig. 2). Therefore, the circulation around the unsteady airfoil can then be determined through integrating the mean velocity around the airfoil.

There is much higher momentum transfer in the upper portion of the wake than in the lower portion of the wake, as indicated by the Reynolds stress distribution (Fig. 3). From the Reynolds stress profiles, it is obvious that the nonzero fluctuating turbulence quantities only exist within the thin viscous wake. No turbulence production appears in the inviscid portion of the wake.

The plunging airfoil undergoes periodic motion. The velocity traces contain a deterministic part, due to the periodic oscillation, and a random part, due to the turbulence. Through ensemble averaging, the deterministic part of the signal can be recovered, whereas the random part of the signal is suppressed. In the present experiment, about 150 ensembles were used in the averaging process. The phase-averaged velocity traces are obtained at many positions across the entire wake. The phase-averaged wake profile at a certain phase can be constructed by cross plotting the velocity traces. The wake profiles for every 60-deg phase difference are shown in Fig. 4. The transverse displacement of the wake following the movement of the airfoil is obvious in the diagram. All of the profiles have an approximately asymmetric bell shape. Since the nominal angle of attack is small and the changes in instantaneous angle of attack are also relatively small, the dynamic stall does not occur on the plunging airfoil and the variation of the wake profile is not very pronounced. However, the phase-averaged wake profiles are not identical at each phase angle, because the instantaneous drag and the momentum integral around the airfoil vary with time. The combination of these two factors results in the variations in the phase-averaged profiles.

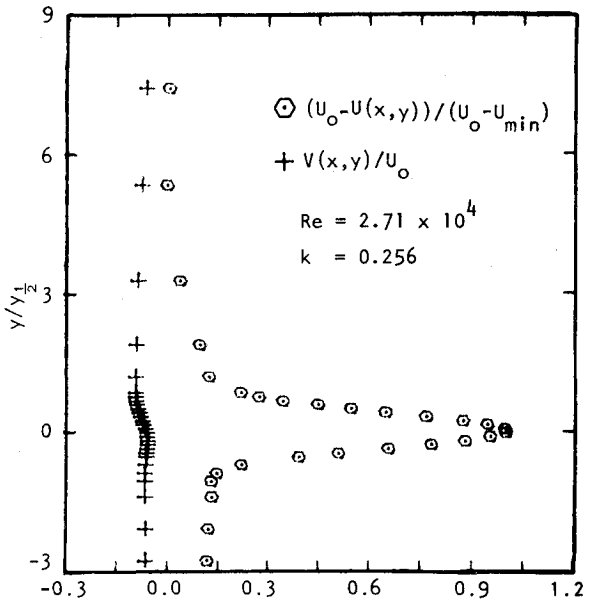

Fig. 2 The profiles of streamwise and transverse velocities.

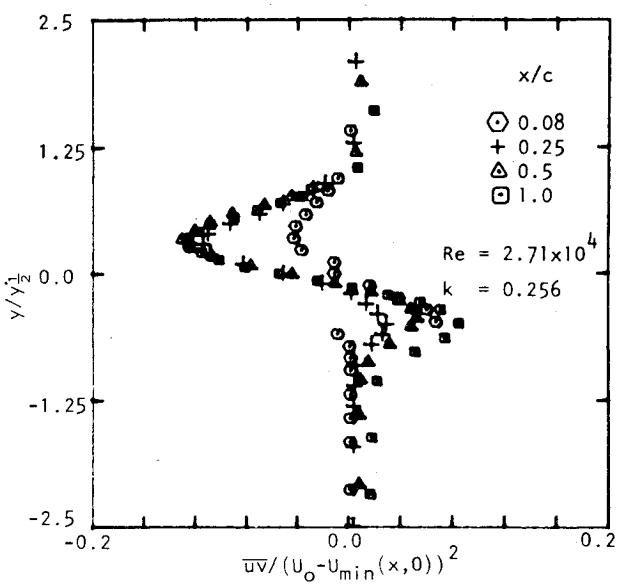

Fig. 3 The Reynolds stress.

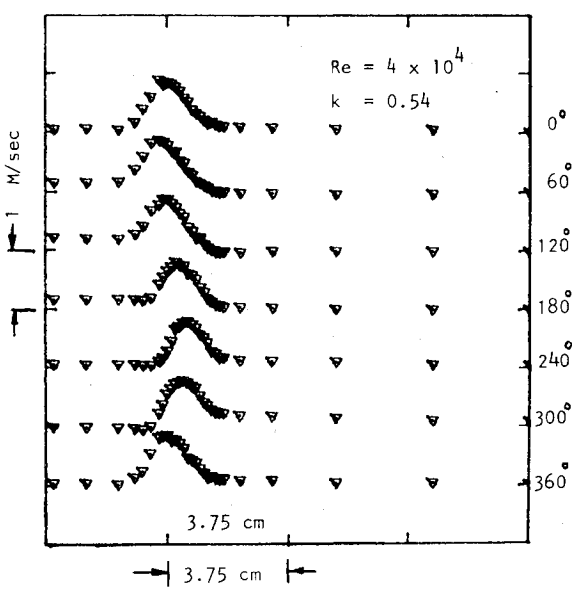

Fig. 4 The profiles of phase-averaged wake.

Conclusion

The preliminary results of the investigation of a plunging airfoil without dynamic stall have revealed several interesting features of the unsteady wake. The near wake consists of a laminar portion and a turbulent portion. The laminar portion is caused by the induced flow of the circulation around the airfoil. The magnitude of the velocity defect is less than 10% of the maximum velocity defect at the center of the wake, but the width is very large compared with the width of the turbulent portion. Thus, the streamwise momentum deficit of the laminar portion of the wake cannot be neglected. The simultaneous measured velocity traces and the Reynolds stress distribution indicate that the unsteady wake has quite different turbulent structures in the upper and lower parts of the wake. The mean transverse velocity was accurately measured. The variations in the circulation during a cycle of oscillation were then obtained by integrating the velocities around the plunging airfoil. The phase-averaged wake profiles are different at different phase angles due to the instantaneous changes in drag and momentum integral around the airfoil.

Acknowledgment

This work was supported by the U.S. Army Research Office under Contract No. DAAG-29-78-G-0073.

References

[1] McCroskey, W. J., "Recent Developments in Dynamic Stall," *Symposium on Unsteady Aerodynamics*, Vol. 1, Univ. of Arizona, March 1975, pp. 1-34.

[2] Fujita, H. and Kovasznay, L.S.G., "Unsteady Lift and Radiated Sound from a Wake Cutting Airfoil," *AIAA Journal*, Vol. 12, Sept. 1974, pp. 1216-1221.

[3] Ho, C. M. and Kovasznay, L.S.G., "Sound Generation by a Single Cambered Blade in Wake Cutting," *AIAA Journal*, Vol. 14, June 1976, pp. 763-766.

[4] Satyanarayana, B., "Unsteady Wake Measurements of Airfoils and Cascades," *AIAA Journal*, Vol. 15, May 1977, pp. 613-618.

[5] Ho, C. M. and Chen, S. H., "Unsteady Wake of a Plunging Airfoil," AIAA Paper 80-1446, Snowmass, Colo., July 1980.

AIAA 81-4301

Two-Dimensional Transonic Nozzle Flows with Shock

C.Q. Lin* and S.F. Shen†
Cornell University, Ithaca, N.Y.

Introduction

IN existing analytical studies of two-dimensional and axially-symmetric transonic nozzle flow problems (for example, see the survey paper of Hall and Sutton[1]), the presence of a shock has yet to be included in the representation. It is believed that, however specialized or limited in scope, such a solution should be valuable from both the basic viewpoint and as a check of various computational methods based upon discretization. The present Note gives an analytical treatment of two-dimensional nozzle flows with shock by expanding the perturbation velocity potential into a double power series. Specifically, an exact solution of the transonic small perturbation equation is continued across a given shock wave and the nozzle shape after the shock is determined as a consequence. Details are worked out for a parabolic shock. The tedious computation for the coefficients of the higher-order terms in the series is performed by computer. The accuracy of the series solution is assessed by evaluating the local residuals. The region of convergence is then considerably enlarged by using the Euler transformation on both coordinates. An illustrative numerical example is given.

Received Jan. 20, 1981; revision received April 13, 1981.

*Visiting Fellow; permanently, Professor, Northwestern Polytechnical University, Xi'an, China.

†Professor, Sibley School of Mechanical and Aerospace Engineering.

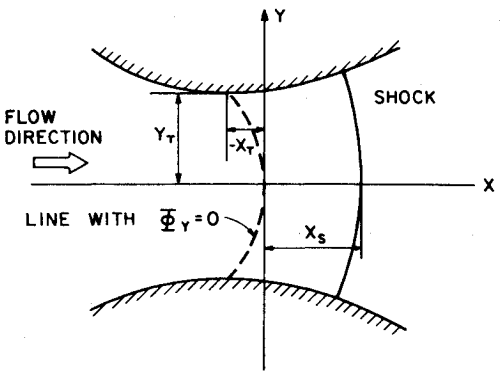

Fig. 1 Nozzle geometry and coordinate system.

Governing Equation and the Solution before the Shock

The Cartesian coordinate system (X, Y) is shown in Fig. 1. We consider a nozzle symmetrical about the X axis and the origin is taken at the sonic point. The transonic small perturbation equation is

$$a^*\Phi_{YY}=(\gamma+1)\Phi_X\Phi_{XX} \tag{1}$$

where Φ is the perturbation velocity potential, a^* the critical speed, and γ the ratio of specific heats. Before the shock, if the velocity along the X axis varies linearly with X, the exact solution of Eq. (1) is well known,[2]

$$\Phi=c\left\{\frac{1}{2}X^2+\frac{1}{2}(\gamma+1)\frac{c}{a^*}XY^2+\frac{1}{24}(\gamma+1)\frac{c^2}{a^{*2}}Y^4\right\} \tag{2}$$

where c is a constant specifying the amplitude of the perturbation velocity. The associated nozzle-wall shape satisfies the tangency condition

$$\frac{dY}{dX}=\frac{\Phi_Y}{a^*+\Phi_X} \tag{3}$$

Let the wall shape be expressed by the series

$$\bar{\eta}=b_0+\sum_{j=2}^{\infty}b_j\bar{\xi}^j \tag{4}$$

with

$$\bar{\xi}=\frac{cX}{a^*}+\frac{\gamma+1}{6}\left(\frac{cY}{a^*}\right)^2 \quad \text{and} \quad \bar{\eta}=(\gamma+1)\left(\frac{cY}{a^*}\right)^2 \tag{5}$$

The line $\bar{\xi}=0$, along which $\Phi_Y=0$, now passes through the throat position. The coefficient b_0 is related to the throat width Y_T, since at $\bar{\xi}=0$ in Eq. (4)

$$b_0=\bar{\eta}_T=(\gamma+1)(c^2Y_T^2/a^{*2}) \tag{6}$$

The recursion formula for the coefficients b_{j+1} $(j=1,2,3,\ldots)$ is omitted for brevity. The constant c and the radius of